# Lab on a Chip

Accepted Manuscript






ROYAL SOCIETY OF CHEMISTRY

www.rsc.org/loc

Journal Name

RSCPublishing

ARTICLE

# Infection and immunity on a chip: A compartmentalised microfluidic platform to monitor immune cell behaviour in real time

Cite this: DOI: 10.1039/x0xx00000x

Received 00th January 2014,
Accepted 00th January 2014

DOI: 10.1039/x0xx00000x

www.rsc.org/

N. Gopalakrishnan [a,b], R. Hannam [a], G. P. Casoni [a], D. Barriet[b], J. M. Ribe[b], M. Haug [a] and Ø. Halaas [a]

Cells respond to their environments and self-organise into multicellular assemblies with dedicated functions. The migratory and homing response of cells to soluble ligands can be studied with different techniques, but for real time studies of complex multicellular self-organisation, novel and simpler systems are required. We fabricated a flexible open access microsystem and tested the design by studying cell recruitment from an immune cell reservoir towards an infectious compartment. The two compartments were connected by a network of bifurcated micro channels allowing diffusion of signalling molecules and migration of cells. Bacterial filters were incorporated in the design to prevent bacteria and activated cells from entering the network, permitting migration only from recruitment reservoir. The fabricated microsystem allows real-time continuous monitoring of cellular decision-making based on biologically produced gradients of cytokines and chemokines. It is a valuable tool for studying cellular migration and self-organisation in relation to infections, autoimmunity, cancer, stem cell homing, tissue and wound repair.

## Introduction

Clearance of infections is a complex process involving many cells and functions over time. Immune system protects organisms from invading pathogens and cancer by reorganising a variety of cells including both immune cells and other cell types like fibroblasts and endothelial cells. This cellular re-organisation happens both at the site of infection and in primary, secondary and tertiary immune organs such as bone marrow, spleen, lymph nodes and local Peyer patches. Tissue-resident dendritic cells (DC) sample their micro-environment and upon activation, migrate into lymph vessels and lymph nodes presenting antigen to naïve T cells and thus priming them to fight the infection [1, 2]. A deeper understanding into these migratory behaviours can thus provide us with a better insight into physiological processes like infections and immunity, but also cancer cell metastasis and stem cell homing[3]. In order to understand these processes and cell assemblies, many *in vivo* and *in vitro* models are employed in which single cellular components are added or removed to predict the outcome of multicellular behaviour [4, 5]. Each model thus provides only a partial picture of the complexity, leaving unresolved gaps. For human-specific infections such as tuberculosis or patient-specific evaluations such as cellular cancer immunotherapy, *in vitro* recreation of immune cell behaviour is possible only when extracorporeal systems with appropriate environments are employed. Hence, novel tools and systems are required to understand the complex cell behaviour and decision making in situ.

Even though 3D matrices have been utilized for cellular self-organization, these systems lack spatial and temporal control [6]. On the other hand, the *in vitro* techniques employed, provides only quantitative measurements of a limited selection of positive and negative regulators in an immune reaction. For example, i*n vitro* studies on cell migration depend on conventional assays including the Boyden chamber[7], Zigmond chamber[8] and subsequent design improvements like Dunn chamber[9] and Insall chamber[10]. Such assays measure the average direction of migration in response to chemical or biological concentration gradients[11]. A major drawback of these conventional techniques is that in these devices, real time visualisation is not possible, cell migration is not polarised and the migratory bias is not controlled (lack of internal controls)[12]. Moreover, the bacteria added as source of infection tends to spread and infect the entire system. Hence, the conventional devices are generic and not tailored for specific purposes.

Recently, many microfluidic approaches which could control the overall architecture, tailor-make and isolate events, has been used to answer the central immunological questions. Wang *et al.* demonstrated a microfluidic wound healing assay, where cells were aligned using channels, reducing sampling volume

[a] Dept. of cancer research and molecular medicine, Norwegian University of Science and Technology, 7489 Trondheim, Norway

[b] NTNU Nanolab, Norwegian University of Science and Technology, 7489 Trondheim, Norway

†Electronic Supplementary Information (ESI) available: [details of any supplementary information available should be included here]. See DOI: 10.1039/b000000x/

and processing time compared to traditional wound-healing assays[13]. Tong *et al.* on the other hand, assembled a microfluidic migration chamber at a single cell resolution for direct visualisation of chemotaxis[14]. Tay's and Whiteside's groups study cell migration and other cell behaviour using microfluidic gradient generators and micropatterns[15, 16]. Nery *et al.* report a microfluidic chamber allowing vectorial cell migration to compare migration velocity and distances [17]. In recent years, there has also been focus on understanding cell decision making. Ambravaneswaran *et. al* explore neutrophil decision making using channels with unequal path lengths[18]. Most of the available solutions hence provide, quantitative control over one or two parameters compared to experiments with petri dishes[19, 20]. Even then, these flow based approaches form an expensive alternative for the use and throw assays widely being used in *in vitro* studies. Moreover, the directional decision making towards biological gradients, inherent to the tissue resident immune cells is not evidently analysed in these devices.

Several challenges still exist to construct *in vitro* models predicting the complex immune cell behaviour in tissue (cellular self-organisation). A simple and flexible cells-on-chip system, closely mimicking complex *in vivo* cell organisation and combining properties of traditional assays could reduce the unresolved gaps. In this work, we describe fabrication and operation of such a device modelling immunological processes as example system. Infection-on-a-chip, mimicking infections and immune reactions: is intended for probing complex immune cell behaviour and decision making. Fig: 1 compares the *in vivo* scenario with the model discussed. We modelled a co-culture platform demonstrating sites of infection by compartmentalising activated tissue resident immune cells and /or bacteria as site of infection and connecting them to recruiting lymphocyte reservoir (~ blood vessel) with channels partially mimicking migration within the tissue.

## Experimental

### Device design and fabrication

The microdevice was fabricated by replica moulding poly(dimethylsiloxane) (PDMS) elastomers onto a silicon (Si) master. The Si master for replica moulding was fabricated using multistep photolithography and dry etching[21]. Fig: 2 shows the schematic of the processes and device fabrication. Channel layouts were designed in CleWin 4 and were printed on chromium based sodalime photomasks obtained from *Compugraphics GmbH*. The Si (110) master was optically patterned (*Suss MA6*, exposure doses: 200mJ/cm$^2$) with channels by spin coating SU-8 5 photoresist (*MicroChem Corp*) at 3000rpm for 30s. The patterns were transferred into the Si substrate using inductively coupled plasma reactive ion etching (ICP-RIE, *Oxford instruments*). An etch rate of 1.7 µm/min was obtained for an RF and ICP power of 50W and 500W respectively. The gas used was a mixture of $SF_6$, $CHF_3$ and $O_2$ with flows of 30sccm, 5sccm and 10sccm respectively[22, 23]. The 10% lateral etch combined with feature size variation exhibit etch depth discrepancies creating a 3D profile to the Si substrate. Extra heights were added to cell loading channels, both in activator and migratory compartments, by realigning and patterning additional photoresist onto the 3D profiled substrate[24].

PDMS devices were prepared by casting a mixture of elastomer and curing agent mixed at a ratio of 10:1 by weight (*Dow Corning* sylgard 184) onto the Si/photoresist master and curing it at 80˚C for 2 hours. Inlets and outlets were punched into the cured PDMS before the devices were plasma bonded ($O_2$:100sccm, 30W, 12s) onto a microscope cover glass (*Menzel Gläser*, Ø 50mm, (No1.5) 150µm thick). The devices were assembled on Willco dishes (7mm side walls) and were immediately filled with deionised (DI) water to retain their surface hydrophilicity[21, 25].

### Cells and materials

**Cell growth:** MF2.2D9 T-cell hybridomas (*Kenneth Rock*, *UMASS*), IC-21 (ATCC TIB-186) macrophages and immortalized B6 macrophages (*Eicke Latz*, *UMASS*) were cultured with RPMI-1640 media containing 10% Fetal Calf serum (FCS), 25mM HEPES, 1.7% L-glutamine, 0.1µM ciprofloxacin, with (and without for macrophages) 50µM 2-mercaptoethanol. Dendritic cells (DC) were generated from C57Bl/6 bone marrow cells by 7 days culture in 20ng/ml GM-CSF (PeproTech) at 1x10$^5$ cells/ml. Dendritic cells were matured (mDC) by 100ng/ml LPS for 24h. Mycobacterium avium (MAV) expressing CFP was cultured as described in Halaas *et. al* [26].

**Cell staining:** Cells were washed 3 times in cold serum-free media before staining with 0.5µM *Molecular Probes® CellTracker™* fluorescent dye (CMFDA) for 45 minutes with frequent mixing at 37°C. Cells were washed three times using complete medium and was allowed to recover overnight before use.

**Antigen presentation assays:** In order to generate inflammatory chemokine gradient, CD4+ MF2.2D9 T-cell hybridomas recognising the ovalbumin 323-339 peptide (ISQAVHAAHAEINEAGR) in complex with I-A$^b$ MHC class II on C57Bl/6 macrophages were pre-incubated with 10µg/ml 323-339 peptide and 100ng/ml Lipopolysaccharide (LPS) for 1-2h. Activated macrophages were detached using 5ml of 0.02% EDTA in PBS and washed twice in complete medium. For antigen presentation, T cells and macrophages/DC were mixed at 3:1 ratio and were loaded onto the devices at the activator side.

**Cell loading in device:**

Prior to cell loading, DI water within the PDMS device was replaced with culture media without FCS and stored at 4˚C overnight. One hour before cell loading, this medium was replaced by complete medium. Cells were re-suspended to a concentration of 2 x 10$^7$ cells/ml whereof 2µl was pipetted into the device. For antigen presentation, unlabelled T-cells were mixed with macrophages/DC at a ratio of 3:1 before loading a volume of 2µl into the activator compartment. Unlabelled, unactivated T-cells (with DC in DC activation experiments) were loaded at the control compartment. Labelled unactivated T-cells/immature DCs (iDCs) were loaded at the migratory compartment.

**Time-lapse microscopy:**

Time lapse fluorescence and differential interference contrast (DIC) images were captured using a 20x objective whilst maintaining devices at 37˚C using *Zeiss LSM 510* inverted confocal microscope with an on-stage incubator. HEPES (25mM) was used to secure pH in devices during measurement

times. Time lapse movies were generated in *Zeiss LSM Image Browser* (v4 2.0.121). Manual cell counts of accumulative migration at regular time-points were obtained from tiled images of the entire network area using tools native to ImageJ (v1.48p).

**Statistical analysis:**
Measures of MF2.2D9 cell migration speed were obtained using time series (*Zeiss LSM* 510) across 5 isolated experiments. A minimum migratory distance of 20μm was used and only net migration in one plane was measured for both confined and free cells. Evaluation of MF2.2D9 decision making at bifurcations was performed from time series taken from multiple devices at different time-points throughout observation, within networks with and without loaded cell mixtures in the activator compartment.
Overall migration of immune cells towards infection was evaluated by comparing number of cells migrated to activator side and control side in 24h. Migration of iDCs towards two different activations were studied for the purpose.

## Results and Discussion

**Preliminary migration experiments**
A rough estimation of the migratory lengths, reaction times and diffusion profiles for microfluidic based chemotaxis assay was determined from preliminary experiments. A device with four different migration lengths was tested. We found that a migration length of 0.5mm (in line with distances between tissue capillaries ~1mm) allowed the formation of cytokine gradients (in the absence of filters) at appropriate times and generated directional cell migration in response to the cell-secreted chemo attractants (data not shown). With suitable migratory and diffusion lengths determined, devices were fabricated with inflammatory foci (compartmentalised and retained in the activator side using multiple 2x2μm filters), separated from the immune cell reservoir (28x100μm) by interconnecting cell-sized channels (6x6μm) (Fig 3a). The channel height profiles measured in a profilometer (*Dektak Profilometer*) is overlaid on to the migratory channel image.

**Simulations**
*Comsol Multiphysics 4.3* was used to simulate the diffusion profiles in the system designed. It was calculated that after 2h of diffusion, migratory reservoir concentration accumulates to 60% of that of the concentration loaded at the activator channel (Fig 3c). The simulation was based on homogeneous transport of diluted species model. The model equation used is time dependent equation:

$$\frac{\partial c}{\partial t} + \nabla.\left(-D\nabla c\right) = 0 \qquad (1)$$

where c is the concentration and D is the diffusion coefficient. The diffusion coefficient used in the simulation was $4.3e^{-10}$ $m^2/s$ [27, 28]. Maximum concentration was set to 10μM. It was inferred from simulations that the molecular gradient developed in the interconnecting network should instigate directional migration of cells from the migratory reservoir towards inflammatory foci within 2-3 hours after the antigen presentation starts. In our devices, the activation of macrophages induces antigen presentation which was expected to occur 2-3 hours after loading cells to the activator compartment.

**Diffusion and filtering**
Cells were loaded carefully in to the loading channels such that cells were not manually injected into the network. This step was ensured so that, presence of cells in the network could only be referred to cell migration. The filters at the activator side withhold both bacteria and cells loaded into the channel, a design criteria creating localised infection (Fig 3a). To check whether the cell debris from the activator compartment would clog the filter and restrict diffusion of chemokines to the network, we monitored permeability and diffusivity of macromolecules with a pre-used cell-loaded old chip by loading 100μM of dextran tetramethyl-rhodamine biotin (DTB) (3kDa). Fig 3b shows the fluorescence gradient obtained from the device immediately after loading DTB, confirming diffusion of molecules through filters to the network. In addition, real time diffusion profiles across the network were checked by loading DTB within a 0.5% diluted viscous methylcellulose solution. It was observed that within 2 hours, DTB diffused and reached the migratory reservoir, as expected from the simulations (Fig 3c, d).

**Cells in the network**We explored and imaged long term cell behaviour in real time using microscopes with heated $CO_2$ incubators. We found that adherent macrophages, non-adherent T cell hybridomas and dendritic cells (not shown) moved freely into and within the network (Supplementary movies 1 (macrophages) and 2 (T cells)), demonstrating suitable micro channel design and choice of material. Cells exhibited migratory speeds of up to 20μm/min and retained migratory phenotypes for several days. The speed of MF2.2D9 cells were comparable to that reported for T-cell *in vivo* migration within the tissues (Fig. 4a)[5, 29]. Due to the seemingly heightened migration ability of MF2.2D9 cell line, we used these T cells as migratory cells in the subsequent experiments.

A major purpose of the network design was to assess decision-making by recruiting cells. We observed that MF2.2D9 cells were twice as likely to maintain their current direction rather than to take a 90° turn at bifurcations (Fig 4b). When encountering such choices within the network, membrane protrusions probed both choices before a decision was made. Cells moved both in and out of the network, communicating with cells in the channel and sometimes moving back into the network. Interestingly a tendency towards common pathways or localising to regions was observed, suggesting favourable physical or biochemical microenvironments or a positive influence of deposited material from preceding cells. It was also evident that the cells interacted with one another in the network. Colliding cells stalled for several minutes before moving together in one direction (Supplementary movie 3). Cell interaction under confinement may thus be exploited for the dynamic study of immunological synapses.

Cells were also able to perform cell-type specific tasks within the network. We observed that macrophages, having caught bacteria (forced into the network), stopped moving during the phagocytic process, whereas adjacent macrophages not directly in contact with the bacteria were unaffected and continued migrating (Supplementary movie 4). When macrophages encountered dead cells within the network, cells immediately stopped moving and started phagocytosing the cell remnants (Supplementary movie 5). From these observations it is clear that our devices can be further adapted for understanding cell

interactions, decision making and memory [30] which is not possible using conventional techniques. Further, the network design is suitable for the study of complex multi-cellular behaviour through real-time tracking of individual cells.

We observed little cell proliferation within the network compared to loading channels which allowed cell division due to their larger dimensions. Cell viability in the devices was comparable to standard culture dishes for the first 24 h and declined steadily afterwards. A few cells were still motile within the network even after 28 days without medium exchange (data not shown).

Further evaluation of the device was performed by loading LPS and immunogenic peptide-loaded macrophages mixed with I-$A^b$-peptide restricted MF2.2D9 cells at 1:3 ratio to the activator compartment (inflammatory focus) and MF2.2D9 cells to the migratory compartment. LPS activates macrophages and results in production of co-stimulatory molecules, pro-inflammatory cytokines and chemokines relevant for most inflammatory and immunological reactions. Fig 4c shows the recruitment kinetics of MF2.2D9 cells over 24 hours towards the activator side. Cells enter the network mostly after 2-3 hours after the loading time. Fig 4d shows a typical tiled image of the cell network of the migrated MF2.2D9 after 24h. Even though for MF2.2D9 T cell hybridoma, directional movement specifically towards inflammation was not so delineating as expected (possibly due to the phenotype of the cell), over the hours, a slight positive migration towards inflammation was observed.

**Immune reactions on a chip**

For MF2.2D9 cell line, we observed little difference in net migration towards inflammatory or unstimulated cell compartments. Hence, instead of MF2.2D9 cell type, we investigated migration of primary dendritic cells towards 1) loaded chemoattractant and 2) on-chip cell-generated gradients. The dendritic cells were not fluorescently labelled to avoid unwarranted activation (data not shown), as these cells are notoriously sensitive to handling. Mature dendritic cells (mDCs) move into lymph nodes due to a CCL19/CCL21 gradient[31]. To check the chemotactic property of the devices, we loaded CCL19 as the chemoattractant into the activator compartment. Though the chemical gradient induced from loading CCL19 was diminishing during the experiment, there was a clear directional migration of mDC towards the CCL19-loaded activator channel compared to medium filled control channel (Fig 5a).

The device was intended for on-chip production of dynamic and complex cell-produced chemokines and cytokines from cell co-cultures and immune reactions, resulting from infections and adaptive immune reactions. We finally evaluated the device by loading the activator compartment with pro-inflammatory or non-activated mDC:Tcell co-cultures showing excellent long term (24h) directional movement of immature DCs (iDCs) towards the activator compartment, confirming the chemotactic function of the device (Fig 5b). We also found a high degree of directional movement of immature DCs (iDC) towards infected dendritic cell compartment (DC+infection), confirming that the compartmentalization worked as intended by retaining bacteria from the network (Fig 5c). It is now possible to probe the effect of cellular contributions in recruitment of new cells, both towards inflammatory foci for immune reactions and towards micro niches in secondary immune organs as well as for cancer, stem cell homing and extravasation from complex cell mixtures in real time.

We are currently redesigning the device based on our findings in order to further increase the potential for the production of potent and dynamic biologically produced chemoattractant gradients.

## Conclusion

Many aspects of our immune system are determined by migratory responses of immune cells, where cells show seek-and-migrate behavior in response to a number of external directional cues. A better insight to such migratory behaviors can elucidate physiological processes underlying infections and immune responses. Traditional approaches cannot be easily tailored to provide real-time observation of the reactions occurring in such complex scenarios. The microfluidic platform that we have developed can mimic the size constraints of physiological environments and provide appropriate chemical cues to generate a better model of cellular immune responses. Unlike available microfluidic techniques where temporally stable gradients are produced by flow of pro-inflammatory cytokine production, our device depends on live cell immune reactions closely mimicking *in vivo* conditions with varied and multiplexed release of chemotactic mediators[14, 18].

In this work, the *in vivo* processes of cell decision making and migration in immune responses are transferred to an experimental format that allows for real time analysis[32]. The interconnecting networks that confine cells while they migrate under the guidance of chemical gradients not only circumvent flow issues brought on by debris or dead cells, but also provides opportunities for studying cellular decision making. Unlike conventional flow based systems, spatial-temporal gradient and size proximity to cells make this no-flow based system an optimal platform for understanding migratory behaviour. Moreover, the diffusion based gradient generation is cost effective in terms of chemokine consumption and is tunable and more relevant to *in vivo* scenarios. Compartmentalising infections using filters at specific sites serve in mimicking infectious foci as well as in simplifying measurement of cell migration as a response to a chemokine gradient. The concept of on-chip reactions makes these devices flexible in terms of potential applications and can be further adapted for cancer metastasis, immunotherapy, tissue remodelling, stem cell homing and many more[33]. This work is supportive of efforts to implement non-animal alternatives to complex multicellular biological processes. We therefore assume such devices could be a microfluidic alternative for conventional chemotactic assays.

## Acknowledgement

The Research Council of Norway is acknowledged for the support to the Norwegian Micro- and Nano- Fabrication Facility, NorFab (197411/V30).

## References

1. D. Alvarez, E. H. Vollmann and U. H. v. Andrian, *Immunity*, 2008, 29(3), 325.



 

2. T. R. Mempel, S. E. Henrickson and U. H. v. Andrian, *Nature*, 2004, 8, 154-159.
3. S. N. Mueller and R. N. Germain, *Nature Reviews Immunology* 2009, 9, 618-629.
4. N. Xu, X. Lei and L. Liu, *J. Vis. Exp.*, 2011, 55, e3296.
5. M. J. Miller, S. H. Wei, M. D. Cahalan and I. Parker, *Proceedings of the National Academy of Sciences*, 2003, 100, 2604-2609.
6. L. G. Griffith and M. A. Swartz, *Nat Rev Mol Cell Biol.*, 2006, 7, 211-224.
7. S. Boyden, *J Exp Med*, 1962, 115, 453.
8. S. H. Zigmond, *J Cell Biology*, 1977, 75.
9. D. Zicha, G. A. Dunn and A. F. Brown, *J Cell Sci*, 1991, 99, 769.
10. A. J. Muinonen-Martin, D. M. Veltman, G. Kalna and R. H. Insall, *PLoS ONE*, 2010, 5.
11. J. Li and F. Lin, *Trends in Cell Biology.*, 2011, 21(8 ), 489-497.
12. F. Lautenschläger and M. Piel, *Curr Opin Cell Biol. 2013*, 2013, 25, 116-124.
13. Y. Wang, Z. Chen, L. X, Z. Du, X. Han, X. Yu and Y. Lu, *Electrophoresis* 2012, 33, 773–779.
14. Z. Tong, E. M. Balzer, M. R. Dallas, W.-C. Hung, K. J. Stebe and K. Konstantopoulos, *PLoS ONE*, 2012, 7, e29211.
15. M. Junkin and S. Tay, *Lab on a Chip*, 2014, DOI: 10.1039/C3LC51182K.
16. G. M. Whitesides, *Nature*, 2006, 442.
17. F. C. Nery, C. C. d. Hora, N. A. Atai, E. Y. Kim, J. Hettich, T. R. Mempel, X. O. Breakefielda and D. Irimia, *Journal of Neuroscience Methods*, 2014, 232, 181-188.
18. V. Ambravaneswaran, I. Y. Wong, A. Aranyosi, M. Toner and D. Irimia, *Integr Biol (Camb)*, 2010, 2(11-12), 639-647.
19. S. K. Kim, W. K. Moon, J. Y. Park and H. Jung, *Analyst*, 2012, 137 4062-4068.
20. J. Wu, X. Wuad and F. Lin, *Lab Chip*, 2013, 13.
21. S. K. Y. Tang and G. M. Whitesides, in *Optofluidics: Fundamentals, Devices, and Applications*, ed. L. P. L. Y. Fainman, D. Psaltis and C. Yang, McGraw-Hill companies, 2009.
22. G. S. Oehrlein and Y. Kurogi, *Materials Science and Engineering*, 1998, 24, 153-183.
23. M. D. Henry, Ph.D Thesis, California Institute of Technology, 2010.
24. S. Choi and J. Park, *Biomicrofluidics*, 2010, 4.
25. D. Qin, Y. Xia and G. M. Whitesides, *Nature Protocols*, 2010, 5.
26. Ø. Halaas, M. Steigedal, M. Haug, J. A. Awuh, L. Ryan, A. Brech, S. Sato, H. Husebye, G. A. Cangelosi, S. Akira, R. K. Strong, T. Espevik and T. H. Flo, *J. Infect Dis.*, 2010, 201, 783-792.
27. N. Huang, W. Chen, B. Oh, T. T. Cornell, T. P. Shanley, J. Fu and K. Kurabayashi, *Lab Chip*, 2012, 12, 4093-4101.
28. A. Heeran, C. P. Luo, G. Roth, A. Ganser, R. Brock, K. H. Wiesmueller, W. Henschel and D. P. Kern, *Microelectronic Engineering*, 2006, 83, 1669-1672.
29. T. Katakai, K. Habiro and T. Kinashi, *The Journal of Immunology*, 2013, 191, 1188-1199.
30. S. H. Ngalim, A. Magenau, G. L. Saux, J. J. Gooding and K. Gaus, *Journal of Oncology*, 2010, 2010.
31. B. G. Ricart, Michael T. Yang, C. A. Hunter, C. S. Chen and D. A. Hammer, *Biophys J*, 2011, 101, 2620–2628.
32. G. Faure-Andre, P. Vargas, M. Yuseff, M. Heuze, J. Diaz, D. Lankar, V. Steri, J. Manry, S. Hugues, F. Vacotto, J. Boulanger, G. Raposo, M. Bonon, M. Rosemblatt, M. Piel and A. Lennon-Dumenil, *Science*, 2008, 322.
33. K. Palucka and J. Banchereau, *Nature Reviews Cancer*, 2012, 12, 265-277.

**Figures**

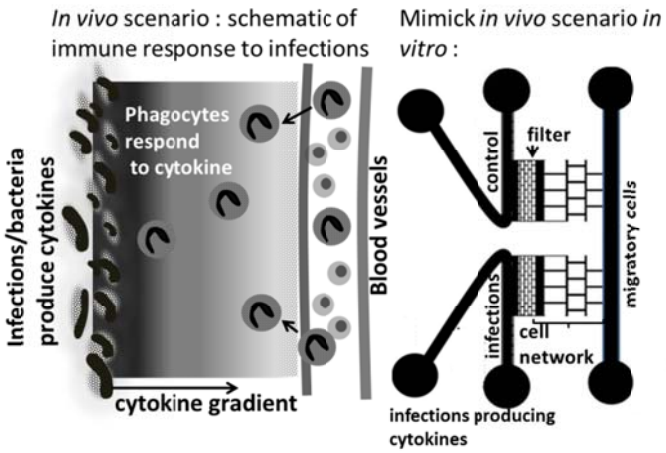


Fig: 1. Mimic *in vivo* scenario *in vitro*: Sites of infections were attained by compartmentalising antigen presenting cells. Cytokine/chemokine diffusing to migratory compartment trigger migratory cell recruitment towards infectious foci.

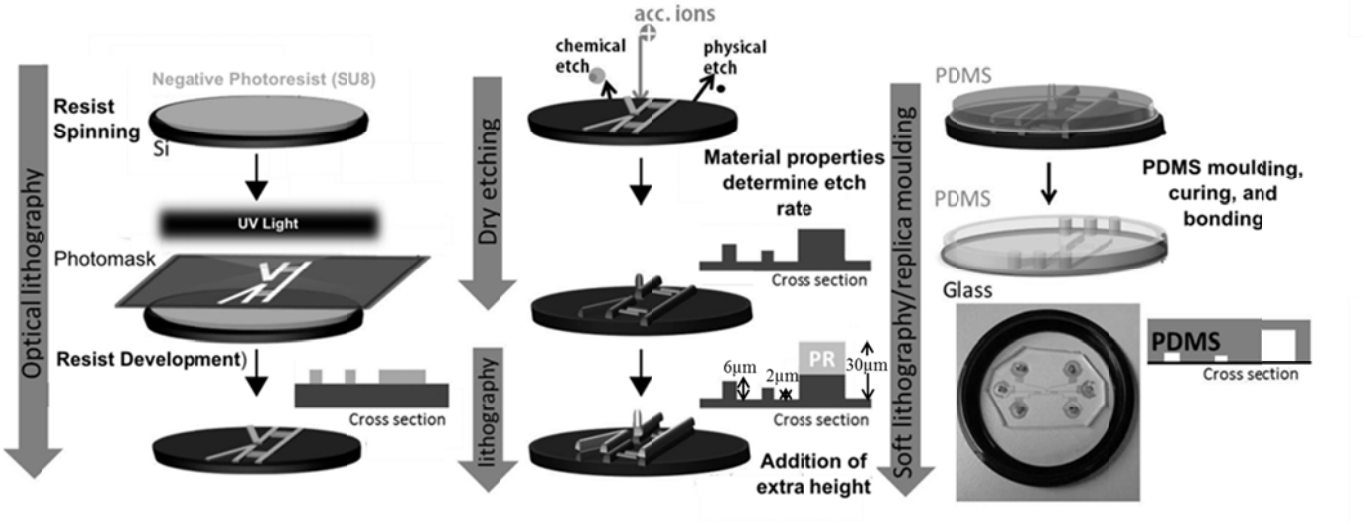


Fig: 2. Schematic of device fabrication: Sites of infections and migratory channels were patterned onto photoresist coated Si master using photolithography. The patterns were transferred to Si using dry etching and additional channel heights were introduced by patterning an extra layer of photoresist. The PDMS based devices were fabricated using replica moulding on Si master.

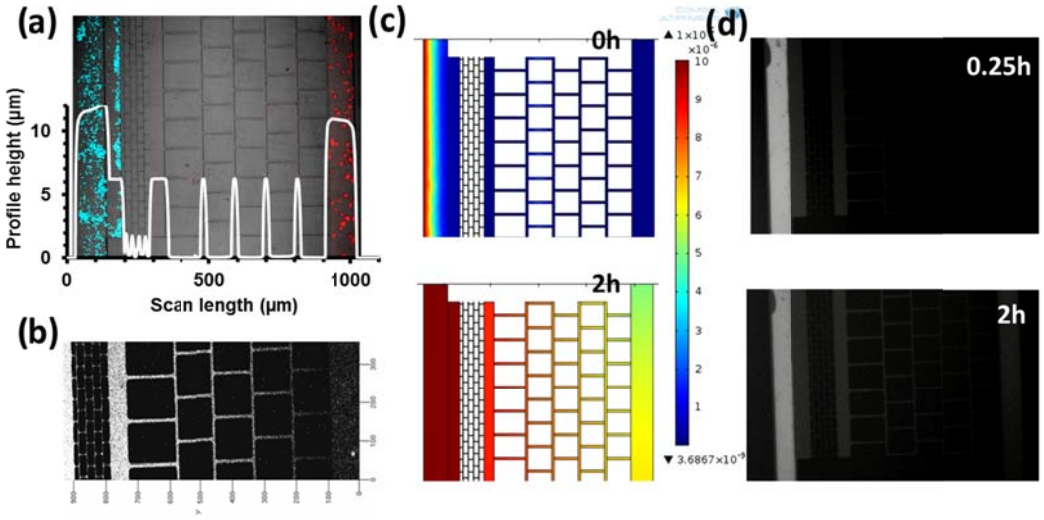


Fig: 3. (a) Infections, CFP stained mycobacterium avium complex is compartmentalized at the activator compartment using filters, while migratory cells were lined up at the migratory compartment (Imaged right after loading cells and infections). These two compartments are connected to one another using networks of cell dimensions. Micro channel profile height is overlaid on to the image. (b) Dextran tetramethylrhodamine biotin (100µM) was used to check filter permeability and diffusivity in used devices. (c, d) Gradient formation: Macromolecule diffusion across the network over time was simulated in COMSOL multiphysics. Diffused DTB (in viscous methylcellulose solution) supports the simulations. It was inferred from diffusion experiments that within 2-3h of chemokine production, cells in migratory compartments should start migrating towards activator compartments.

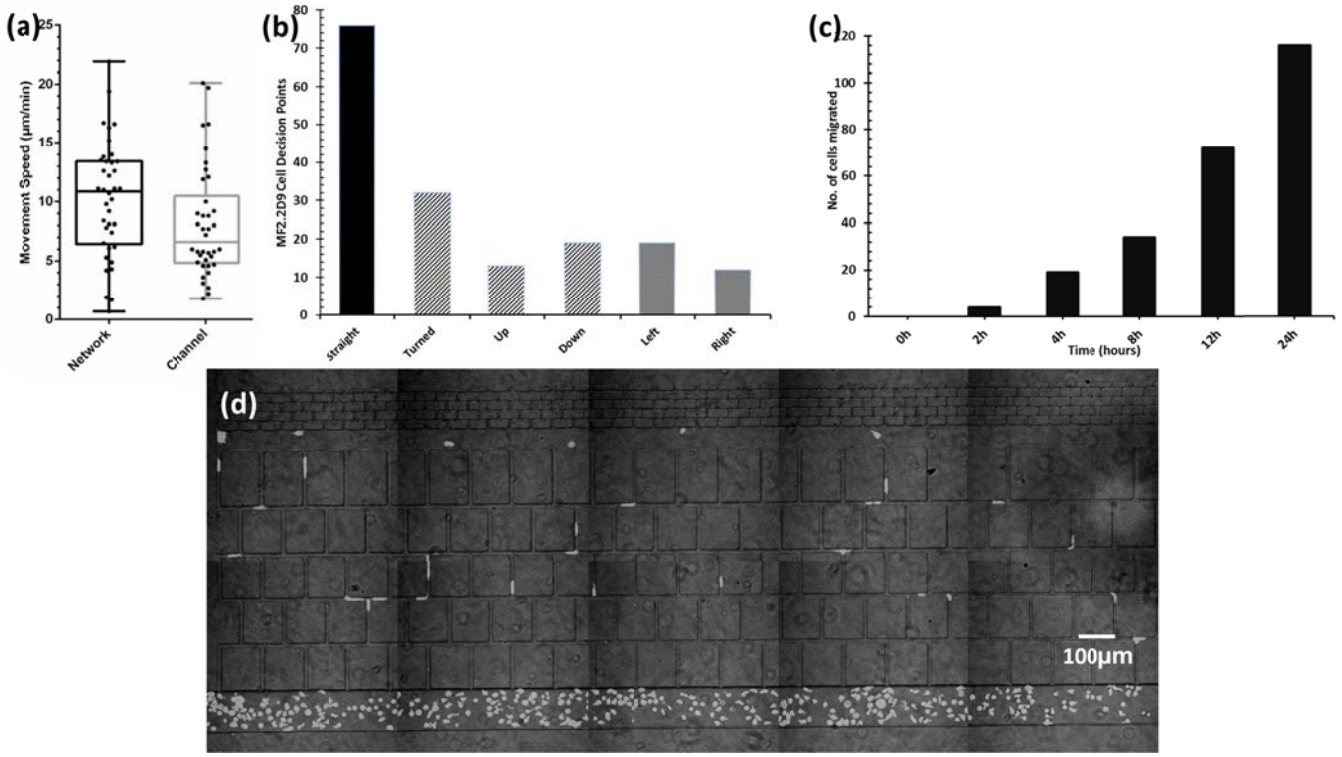


Fig: 4. (a) Cell speed in network vs microchannels (b) MF2.2D9 choices made at bifurcations. Moving straight is assumed as moving parallel to the migratory and activator compartments. Counts were made across multiple devices at the cell network leading towards inflammatory compartments. (c) Migration of CMFDA labelled MF2.2D9 cells over 24 hours towards MF2.2D9 stimulated with LPS and ovalbumin peptide. (d) Tile scan image of CMFDA labelled MF2.2D9 cells entering and migrating within networks towards infections.

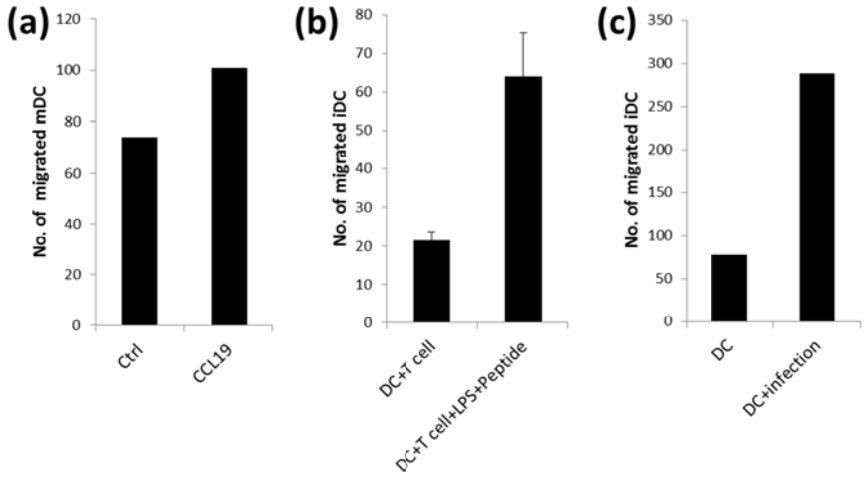


Fig: 5(a) Migration of mDC towards gradients of CCL19. b) iDc migration towards mixtures of DC and MF2.2D9 stimulated with LPS and OVA 323-339 peptide presented as mean-SD of two independent experiment and c) towards mDC stimulated with bacteria. For the data presentation migrating cells are counted at the activator and control side 24h after cells were loaded into the device.